

Cryo-EM structures of the human sodium-potassium pump revealing the gating mechanism on the cytoplasmic side

Yingying Guo

Westlake University

Yuanyuan Zhang

Westlake University

Renhong Yan

Westlake University <https://orcid.org/0000-0002-7122-6547>

Bangdong Huang

Westlake University

Fangfei Ye

Westlake University

Liushu Wu

Westlake University

Ximin Chi

Westlake University <https://orcid.org/0000-0002-3839-5998>

Qiang Zhou (✉ zhouqiang@westlake.edu.cn)

Westlake University

Article

Keywords: Membrane-bound Ion Pump, Post-Albers Cycle, Cytoplasmic Gate, Na⁺ Entrance Pathway

Posted Date: June 3rd, 2021

DOI: <https://doi.org/10.21203/rs.3.rs-557882/v1>

License:   This work is licensed under a Creative Commons Attribution 4.0 International License.

[Read Full License](#)

Version of Record: A version of this preprint was published at Nature Communications on July 8th, 2022. See the published version at <https://doi.org/10.1038/s41467-022-31602-y>.

Abstract

Na^+/K^+ -ATPase (NKA) is a membrane-bound ion pump that generates electrochemical gradient of sodium ion and potassium ion across the plasma membrane via hydrolyzing ATP. During each so-called Post-Albers cycle, NKA exchanges three cytoplasmic sodium ions for two extracellular potassium ions through alternating E1 and E2 states. Hitherto, there are several steps remained unknown during the complete working cycle of NKA. Here, we report cryo-electron microscopy (cryo-EM) structures of recombinant over-expressed human NKA in three distinct states at 3.1–3.4 Å resolution, representing the E1·3Na state, in which the cytosolic gate is open, and the E1·3Na·ATP state preceding ATP hydrolysis and a basic E2·[2K] state. These structures reveal the ATP-dependent Na^+ -binding site remodeling for the close of the cytoplasmic gate, filling a gap in the structural elucidation of the Post-Albers cycle of NKA and providing structural basis for understanding the cytoplasmic Na^+ entrance pathway.

Introduction

The sodium potassium pump (Na^+/K^+ -ATPase, NKA) is expressed in the plasma membrane of all animal cells and belongs to the P-type ATPase family¹⁻³. NKA converts energy derived from ATP hydrolysis into electrochemical potential gradient of Na^+ and K^+ across the plasma membrane, which is required for numerous physiological processes⁴. NKA undergoes an ATP-driven transport cycle called Post-Albers scheme (Supplementary Fig. 1)^{5,6}, during which NKA exchanges three cytoplasmic Na^+ ions for two extracellular K^+ ions through transition between the inward-facing E1 state and the outward-facing E2 state coupled with hydrolysis of one ATP molecule. The E1 state of NKA has a higher affinity to Na^+ , while the E2 state has a higher affinity to K^+ .

NKA consists of a large multi-transmembrane catalytic α subunit, a single transmembrane β subunit, and an auxiliary γ subunit called FX γ D. There are four, three and seven isoforms for α , β and γ subunit of human NKA (hNKA), respectively. The α subunit contains ten transmembrane helices (M1-M10) and three cytosolic domains: the actuator (A) domain, the nucleotide-binding (N) domain, and the phosphorylation (P) domain. The A, N, and P domains of α subunit form the cytoplasmic headpiece, which undergoes cycles of phosphorylation and dephosphorylation, resulting in closed and opening headpiece conformation, respectively^{6,7}. Early reported crystal structures of pig and shark NKA E2·P and E2·Pi with and without cardiotonic steroids provided valuable information for the understanding of extracellular cation pathway⁸⁻¹². ATP binds to the N domain¹³ facilitated by a Mg^{2+} cofactor to phosphorylate an aspartate residue in the P domain, forming an aspartyl-phosphorylated intermediate state (E1~P·[3Na]·ADP, Protein Data Bank (PDB) codes: 3WGU¹⁴ and 4HQJ¹⁵) with three cytoplasmic Na^+ occluded. NKA undergoes large conformational changes during Na^+ access to the ion-binding sites and occluded by cytoplasmic gate closing. Therefore, questions are remained that how cation exchanges from cytoplasmic route and what is the gating mechanism on the cytoplasmic side.

Results

Structural determination of hNKA in three conformations

To solve the human NKA (hNKA) structure and investigate the cytoplasmic gating mechanism, we overexpressed and purified hNKA that contained $\alpha 1$, $\beta 1$ and $\gamma 2$ subunits (Supplementary Fig. 2a). To trap hNKA in the E1 state, only Na^+ and Mg^{2+} were added in buffer when purification¹⁶. In the same way, existence of only K^+ in solution can stabilize the conformation in E2 state¹⁶. We determined the cryo-EM structures of hNKA in three conditions: 1) 150 mM NaCl, 3mM Mg^{2+} , 1 mM ATP analogue (adenosine 5'-O-(3-thio) triphosphate, ATP γ S), 2) 150 mM NaCl, 3mM Mg^{2+} , and 3) 100 mM KCl, 3mM Mg^{2+} (Supplementary Fig. 2-4 and Supplementary Table 1). The cryo-EM structures solved in these conditions represent E1·3Na·ATP, E1·3Na, and E2·[2K] states with resolution of 3.1, 3.4, and 3.1 Å respectively, good enough for model building and subsequent structural analysis.

Overall structure of the E1 state preceding ATP hydrolysis

We successfully solved the cryo-EM structures of hNKA in the E1·3Na and E1·3Na·ATP state at 3.4 Å and 3.1 Å resolution in the absence or presence of a slowly hydrolyzed ATP analogue, respectively, representing two E1 structures of hNKA preceding ATP hydrolysis previously unknown according to our knowledges. Intriguingly, we observed an opening K^+/Na^+ -exchanging path in our E1 state structures between transmembrane Na^+ -binding site and cytoplasm (Fig. 1, Supplementary Movie 1).

The structures of the E1·3Na·ATP and E1·3Na states are virtually identical with a root mean square deviation (RMSD) of 0.348 Å, except a slightly difference in ATP binding pocket in the cytoplasmic headpiece and the Na^+ -binding sites in transmembrane region of $\alpha 1$ subunit (Fig. 2 and Supplementary Fig. 5). We found that the configuration of cytosolic headpiece of NKA changes in E1 state. Both the E1·3Na·ATP and E1·3Na structures are in open headpiece conformation, in which the A domain is separated from the N domain and stabilized only by the eighth helix at the end of the P domain (Pa8), (Supplementary Fig. 5a, asterisks location). In the E1~P·[3Na]·ADP state (PDB code: 3WGU), in which ATP is hydrolyzed to ADP but not released, the A domain interacts with the N domain with two additional sites (Supplementary Fig. 5a, plus symbols), stabilizing the closed conformation of the headpiece¹⁴. The movement and rotation of the A domain pull up the M1 helix after phosphorylation, to close the cytoplasmic gate (Fig. 3a).

In E1·3Na·ATP and E1·3Na states, NKA have three Na^+ -binding sites I, II and III, which are located in the middle of the membrane (Fig. 1 and 4a-c). As compared with the E1~P·[3Na]·ADP state of pig NKA, the

positions of three Na⁺ are different (Fig. 4d-f), of which site α and β locations are changed largely and site γ seems very restricted throughout the E1 basic state (Fig. 4e,f; Supplementary Fig. 5b, c). During the E1·3Na/E1·3Na·ATP to E1~P·[3Na]·ADP transition, Na⁺-binding sites move toward the depth of cation binding cavity (Fig. 4e, f).

The cytoplasmic gate closure coupled with ATP hydrolysis

In the physiological situation, the binding of ATP accelerates the transition from E2·[2K] to E1 state^{4,5}. During this process, the cytoplasmic gate of NKA must open for releasing K⁺ to the cytoplasm and then fill transmembrane Na⁺-binding sites sequential with three intracellular Na⁺^{14,17}. Then the cytoplasmic gate close and three Na⁺ are occluded within the NKA. Our samples reveal two similar E1 states (E1·3Na and E1·3Na·ATP) structures preceding ATP hydrolysis with opening cytoplasmic pathway (Fig. 1, 2, Supplementary Fig. 5b). Compared to the E1·3Na·ATP state, large conformational changes are observed in the E1~P·[3Na]·ADP state (Fig. 3a). The closing of the cytoplasmic headpiece induces the closing of the M1 sliding door and occlusion of the bound Na⁺. ADP has a smaller pocket by the tilt with N and P domain aligning with P_N (Fig. 3b, c). These changes bring the A domain further toward the N domain and close the headpiece (Fig. 3a, Supplementary Fig. 5a). As a result, gate closing signal would be transmitted to the A domain sit on Pa8 helix and make it rotates about 26° to pull up the M1 sliding door (Fig. 3a red arrow). Notably, M1e is moved towards the cytoplasmic side for about 5 Å, and close NKA cytosolic door directly (Supplementary Fig. 5c).

ATP binding and hydrolysis adjust the sodium ion binding sites

E1·3Na and E1·3Na·ATP are largely similar. However, it seems evident that the reaction with ATP causes different extents of rearrangements of the three Na⁺. Na⁺ in site α and β of E1·3Na and E1·3Na·ATP states are juxtaposed at the interhelix space between M4-M6, and closer to the cytoplasmic surface (Fig. 4a-c). We observe a gate residue Glu334 on M4e at the door, whose orientation of side chain tends to open and close accompanied by M1 sliding door conformational changes (Fig. 4d-f). Glu334 (Glu327 in pig) only coordinate site α Na⁺ to help close the cytosolic door when ATP hydrolysis to ADP (Fig. 4d). Glu334 is highly conserved among P2-ATPases (Supplementary Fig. 10). The side chains of Asp811 and Asp815 (Asp804 and Asp808 in pig) in M6 are play an important role in site α and β formation. Asp811 side chain coordinates site α Na⁺ at E1·3Na state but stabilizes site β Na⁺ when it moves deeper in E1·3Na·ATP state (Fig. 4b,c). Obviously, the Na⁺ of site β is the initial binding at the deepest position of funnel shaped Na⁺-binding cavity, and site α Na⁺ is the last one binding near the gate. This Na⁺ ions binding sequential scenario is in good agreement with the hypothesis in pig NKA E1~P·[3Na]·ADP state structure studies¹⁴.

All Na⁺-binding sites are slightly offset to the M5 and M8 side during E1·3Na/E1·3Na·ATP to E1~P·[3Na]·ADP transition, raising the question how the ATP binding and hydrolysis affect the Na⁺-binding site. Indeed, ATP and Na⁺ bind to spatially distant locations from cytosolic headpiece to transmembrane domain. The binding of ATP induces rotation of the N domain for about 7° (Fig. 2a) with Arg692 on the short loop connecting the third strand (Pβ3) and the sixth helix (Pα6) functioning as a pivot (Supplementary Fig. 6a). The adenine ring of the bound nucleotide is stacked with Phe482, and interacts with Glu453, Asp450 and Arg551 (Fig. 2d). The γ-phosphate of ATPγS inserts into the P domain, stabilized by a cofactor Mg²⁺, Thr378 and Gly618 (Fig. 2b, d), decreasing distance between the N domain and the P domain. As a result, ATP analogue is delivered to the phosphorylation site with a proper orientation that facilitates phosphoryl transfer. In E1·3Na, Mg²⁺ stabilizes the important ³⁷⁶DKTGTLT motif and the ⁷¹⁵TGDGVND motif (Fig. 2c). The ATP binding changes the location of cofactor Mg²⁺ (Fig. 2e), disrupting the hydrogen bond network formed with these two motifs. These changes make ³⁷⁶DKTGTLT motif loosely and move subtly (Fig. 2e arrow; Supplementary Fig. 6b), which is connected to M4 through Pβ1, Pα1, Pβ0 and interacts with Pβ6-Pα8, Pβ7-M5 loops near M5 (Supplementary Fig. 6b, c). Therefore, ATP binding induce conformational changes in ³⁷⁶DKTGTLT motif and affects the binding of cofactor Mg²⁺ and might trigger the orientation of M4 and M5 and adjust the position of the Na⁺-binding sites. The binding of ATP coupled with the movement of M4 and M5 might result in the displacement of Na⁺-binding site (Supplementary Fig. 6c). The rearrangement three Na⁺-binding site to move toward the depth of cation binding cavity is to prepare for the next step to close the inner cell door (Fig. 4). After binding of three Na⁺ and ATP molecule, M1 sliding door rearranges to a position that blocks the cytoplasmic entrance pathway.

K⁺-occluded E2 basic state

In addition to the E1·3Na·ATP and E1·3Na structures described above, we also obtained a cryo-EM structure of hNKA in the E2·[2K] state at 3.1 Å resolution (Supplementary Figs. 1), which is a basic state following dephosphorylation with two K⁺ ions in occluded conformation (Fig. 5a, b). A cytoplasmic K⁺ site (Site C) is the third K⁺-binding site (Fig. 5a, red circle), which is implicated in activation of dephosphorylation¹⁸. As compared to the E2·[2K]·Pi state (a preceding state in Post-Albers cycle, Supplementary Fig. 1; PDB code: 3KDP)⁸, the two structures are very similar with an RMSD of 1.087 Å (Supplementary Fig. 7a). The K⁺-binding sites I and II between the M4, M5 and M6 are almost identical (Supplementary Fig. 7b). K⁺-coordinating residues at site I (Asp815, Asp811, Ser782, Glu786 and Asn783) and site II (Asp811, Glu334, Val332, Val329, Ala330 and Asn783) are similar to that of Na⁺-binding site I and II in corresponding E1·3Na·ATP state (Fig. 2b, Supplementary Fig. 7b, 8b). The ²¹⁹TGES motif of A domain, which plays important role in dephosphorylation of E2P to E2 transition¹⁹⁻²¹, is further stabilized by Mg²⁺ and ³⁷⁶DKTGTLT motif in P domain (Fig. 5c, d, Supplementary Fig. 7c, d). Compared with E1·3Na·ATP state, the α1 subunit undergoes a large conformational change (Supplementary Fig. 8). In TM region, M1 to M6 rotate toward the opposite side for about 20°, whereas M7 to M10 are relatively

rigid. When the P_N domain is aligned, the N domain tilts for 99° , and the A domain rotates for about 71° relative to $E1 \cdot 3Na \cdot ATP$ state (Supplementary Fig. 8a). From the $E2 \cdot [2K]$ to $E1 \cdot 3Na \cdot ATP$ state, the $^{219}TGES$ motif moves for 11.7 \AA to expose the conserved Asp376 phosphorylation site (Supplementary Fig. 8c).

Discussion

P-type ATPases share similar structural architectures and common mechanisms of substrate transport using domain-association moving parts coupled with ATP hydrolysis to conformational change²². P-type ATPases superfamily can be classified into 11 subfamilies, among which subfamily II comprises NKA and Ca^{2+} -ATPases in mammals^{2,3}. The structure of $E1 \cdot Mg^{2+}$ state of Ca^{2+} -ATPase with an opened cytoplasmic gate has been reported²³. The binding of Ca^{2+} and ATP bends P domain, changes location of N and A domain, and induces closing of cytosolic headpiece, so that the rotation of A domain pulls up M1 and close M1 sliding door (Supplementary Fig. 9)²⁴⁻²⁷. In $E1 \cdot 3Na \cdot ATP$ state of NKA reported in this work, the cytoplasmic headpiece remains opened when both Na^+ and ATP are bound (Fig.3a). The M1 moves to cytoplasm to close the cytoplasmic gate and form the occluded conformation accompanying the closing of headpiece when ATP is hydrolyses to ADP in NKA^{14,15}. These observations indicate that occluded conformation of NKA is coupled to ATP hydrolysis rather than ATP binding.

There are more than 30 crystal structures of NKA have been published, revealing the multiple states in Post-Albers Cycle. To compare these structures, we calculated paired RMSD values for all of NKA structures (Supplementary Fig. 11), based on which two major states representing E1 and E2 state are revealed. The $E1 \cdot 3Na \cdot ATP$ and $E1 \cdot 3Na$ structures in this work belong to E1 state that contains another 3 structures in $E1 \sim P \cdot [3Na] \cdot ADP$ state. The E2 state includes the most structures (85%) that can be classified into two states, $E2 \cdot P$ and $E2 \cdot Pi$. The $E2 \cdot [2K]$ structure in this work is in between the $E2 \cdot P$ and $E2 \cdot Pi$ state but is more similar to $E2 \cdot P$ state. The $E1 \cdot 3Na \cdot ATP$ and $E1 \cdot 3Na$ structures reveal cytoplasmic gating mechanism correlated with the ATP-dependent Na^+ -binding site remodeling (Supplementary Fig. 12, Supplementary Movie 1), providing more essential information to understand the working mechanism of the whole reaction cycle of NKA.

Declarations

Acknowledgments

We thank the cryo-EM facility, the high-performance computing center and the mass spectrometry & metabolomics core facility of Westlake University for providing the supports. This work was supported by the National Natural Science Foundation of China (projects 31800139, 31971123, 32022037).

Author contributions

Q.Z. conceived the project. Q.Z., and Y.G. designed the experiments. Y.G., Y.Z. and R.Y. did the experiments. F.Y., B.H., and L.W. contributed to make figures and movies. All of authors contributed to the

data analysis. Q.Z. and Y.G. wrote the manuscript.

Competing interests

The authors declare no competing interests.

Data and materials availability

Atomic coordinates and cryo EM density maps of the E1·3Na·ATP, E1·3Na and E2·[2K] (PDB code: 7E21, 7E1Z and 7E20; whole map: EMD-30949, EMD-30947 and EMD-30948) have been deposited to the Protein Data Bank (<http://www.rcsb.org>) and the Electron Microscopy Data Bank (<https://www.ebi.ac.uk/pdbe/emdb/>), respectively. Correspondence and requests for materials should be addressed to Q.Z. (zhouqiang@westlake.edu.cn).

References

1. Palmgren, M.G. & Nissen, P. P-type ATPases. *Annu Rev Biophys* **40**, 243-66 (2011).
2. Chan, H. et al. The p-type ATPase superfamily. *J Mol Microbiol Biotechnol* **19**, 5-104 (2010).
3. Axelsen, K.B. & Palmgren, M.G. Evolution of substrate specificities in the P-type ATPase superfamily. *J Mol Evol* **46**, 84-101 (1998).
4. Jorgensen, P.L., Hakansson, K.O. & Karlsh, S.J. Structure and mechanism of Na,K-ATPase: functional sites and their interactions. *Annu Rev Physiol* **65**, 817-49 (2003).
5. Post, R.L., Hegyvary, C. & Kume, S. Activation by adenosine triphosphate in the phosphorylation kinetics of sodium and potassium ion transport adenosine triphosphatase. *J Biol Chem* **247**, 6530-40 (1972).
6. Dyla, M., Kjaergaard, M., Poulsen, H. & Nissen, P. Structure and Mechanism of P-Type ATPase Ion Pumps. *Annu Rev Biochem* **89**, 583-603 (2020).
7. Dyla, M., Basse Hansen, S., Nissen, P. & Kjaergaard, M. Structural dynamics of P-type ATPase ion pumps. *Biochem Soc Trans* **47**, 1247-1257 (2019).
8. Morth, J.P. et al. Crystal structure of the sodium-potassium pump. *Nature* **450**, 1043-9 (2007).
9. Ogawa, H., Shinoda, T., Cornelius, F. & Toyoshima, C. Crystal structure of the sodium-potassium pump (Na⁺,K⁺-ATPase) with bound potassium and ouabain. *Proc Natl Acad Sci U S A* **106**, 13742-7 (2009).
10. Shinoda, T., Ogawa, H., Cornelius, F. & Toyoshima, C. Crystal structure of the sodium-potassium pump at 2.4 Å resolution. *Nature* **459**, 446-50 (2009).
11. Laursen, M., Gregersen, J.L., Yatime, L., Nissen, P. & Fedosova, N.U. Structures and characterization of digoxin- and bufalin-bound Na⁺,K⁺-ATPase compared with the ouabain-bound complex. *Proc Natl Acad Sci U S A* **112**, 1755-60 (2015).
12. Kanai, R. et al. Binding of cardiotonic steroids to Na⁽⁺⁾,K⁽⁺⁾-ATPase in the E2P state. *Proc Natl Acad Sci U S A* **118**(2021).

13. Hilge, M. et al. ATP-induced conformational changes of the nucleotide-binding domain of Na,K-ATPase. *Nat Struct Biol* **10**, 468-74 (2003).
14. Kanai, R., Ogawa, H., Vilsen, B., Cornelius, F. & Toyoshima, C. Crystal structure of a Na⁺-bound Na⁺,K⁺-ATPase preceding the E1P state. *Nature* **502**, 201-6 (2013).
15. Nyblom, M. et al. Crystal structure of Na⁺, K⁽⁺⁾-ATPase in the Na⁽⁺⁾-bound state. *Science* **342**, 123-7 (2013).
16. Jorgensen, P.L. Purification and characterization of (Na⁺, K⁺)-ATPase. V. Conformational changes in the enzyme Transitions between the Na-form and the K-form studied with tryptic digestion as a tool. *Biochim Biophys Acta* **401**, 399-415 (1975).
17. Apell, H.J. & Karlisch, S.J. Functional properties of Na,K-ATPase, and their structural implications, as detected with biophysical techniques. *J Membr Biol* **180**, 1-9 (2001).
18. Schack, V.R. et al. Identification and function of a cytoplasmic K⁺ site of the Na⁺, K⁺ -ATPase. *J Biol Chem* **283**, 27982-27990 (2008).
19. Toyoshima, C. Structural aspects of ion pumping by Ca²⁺-ATPase of sarcoplasmic reticulum. *Arch Biochem Biophys* **476**, 3-11 (2008).
20. Anthonisen, A.N., Clausen, J.D. & Andersen, J.P. Mutational analysis of the conserved TGES loop of sarcoplasmic reticulum Ca²⁺-ATPase. *J Biol Chem* **281**, 31572-82 (2006).
21. Clausen, J.D., Vilsen, B., McIntosh, D.B., Einholm, A.P. & Andersen, J.P. Glutamate-183 in the conserved TGES motif of domain A of sarcoplasmic reticulum Ca²⁺-ATPase assists in catalysis of E2/E2P partial reactions. *Proc Natl Acad Sci U S A* **101**, 2776-81 (2004).
22. Zhang, X.C. & Zhang, H. P-type ATPases use a domain-association mechanism to couple ATP hydrolysis to conformational change. *Biophysics Reports* **5**, 167-175 (2019).
23. Inesi, G., Lewis, D., Ma, H., Prasad, A. & Toyoshima, C. Concerted conformational effects of Ca²⁺ and ATP are required for activation of sequential reactions in the Ca²⁺ ATPase (SERCA) catalytic cycle. *Biochemistry* **45**, 13769-78 (2006).
24. Toyoshima, C., Yonekura, S., Tsueda, J. & Iwasawa, S. Trinitrophenyl derivatives bind differently from parent adenine nucleotides to Ca²⁺-ATPase in the absence of Ca²⁺. *Proc Natl Acad Sci U S A* **108**, 1833-8 (2011).
25. Toyoshima, C. & Mizutani, T. Crystal structure of the calcium pump with a bound ATP analogue. *Nature* **430**, 529-35 (2004).
26. Sorensen, T.L., Moller, J.V. & Nissen, P. Phosphoryl transfer and calcium ion occlusion in the calcium pump. *Science* **304**, 1672-5 (2004).
27. Kabashima, Y., Ogawa, H., Nakajima, R. & Toyoshima, C. What ATP binding does to the Ca⁽²⁺⁾ pump and how nonproductive phosphoryl transfer is prevented in the absence of Ca⁽²⁾. *Proc Natl Acad Sci U S A* **117**, 18448-18458 (2020).

Figures

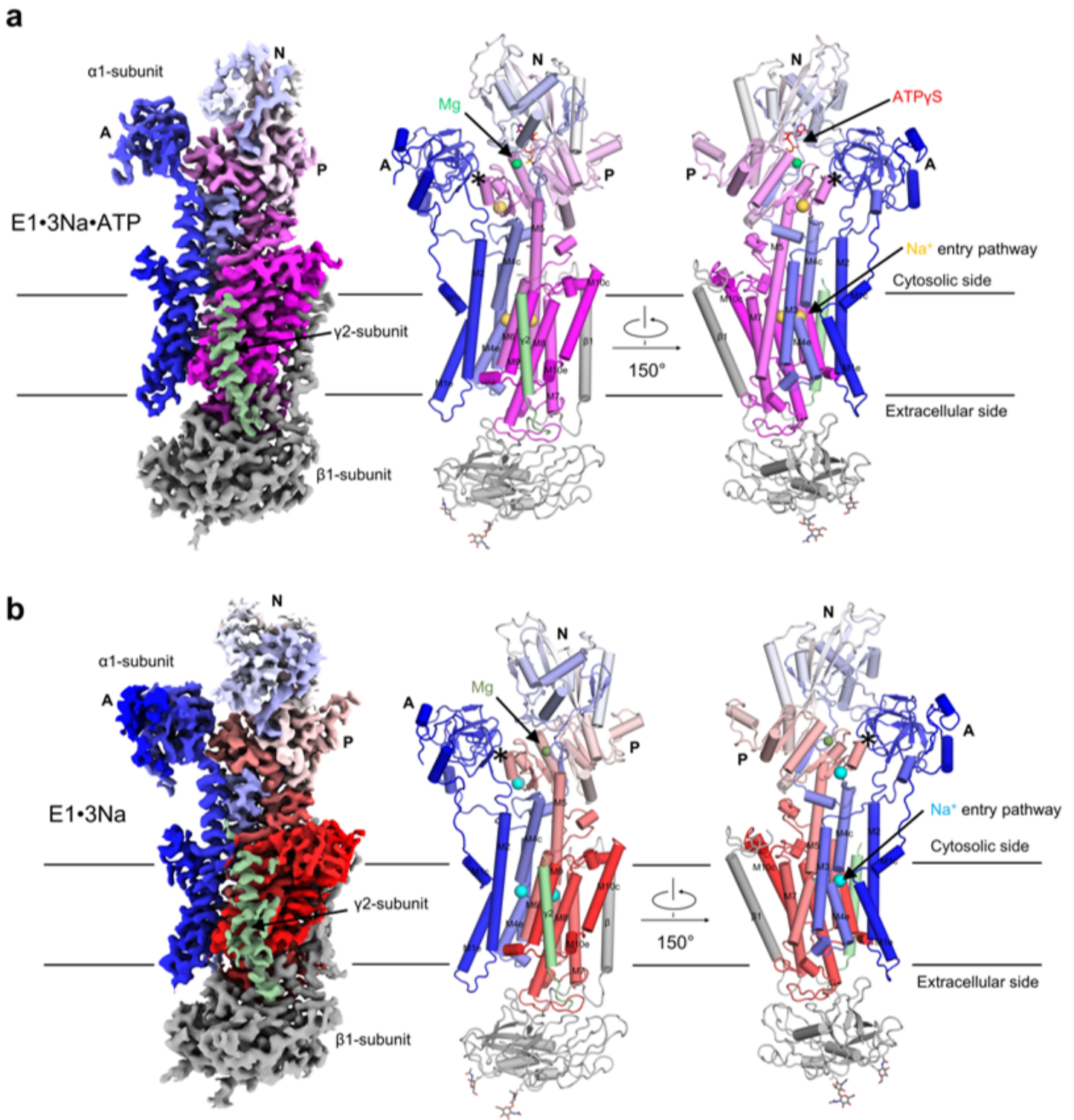


Figure 1

Overall structure of the E1·3Na·ATP and the E1·3Na state. a, The overall cryo-EM map (left panel) and two views of the overall structure (middle and right panel) of the E1·3Na·ATP state. $\alpha 1$ subunit is colored by amino acid sequence with a spectrum from blue to magenta. $\beta 1$ subunit is colored grey. $\gamma 2$ subunit is colored palegreen. b is same to a, but for the E1·3Na state (colored as a spectrum from blue to red). Na⁺ ions are colored yellow or cyan in a or b, respectively. Mg²⁺ ions are colored green or forest green in a or

b, respectively. The glycosylation moieties are shown as sticks. e, extracellular; c, cytosolic; M, transmembrane helix.

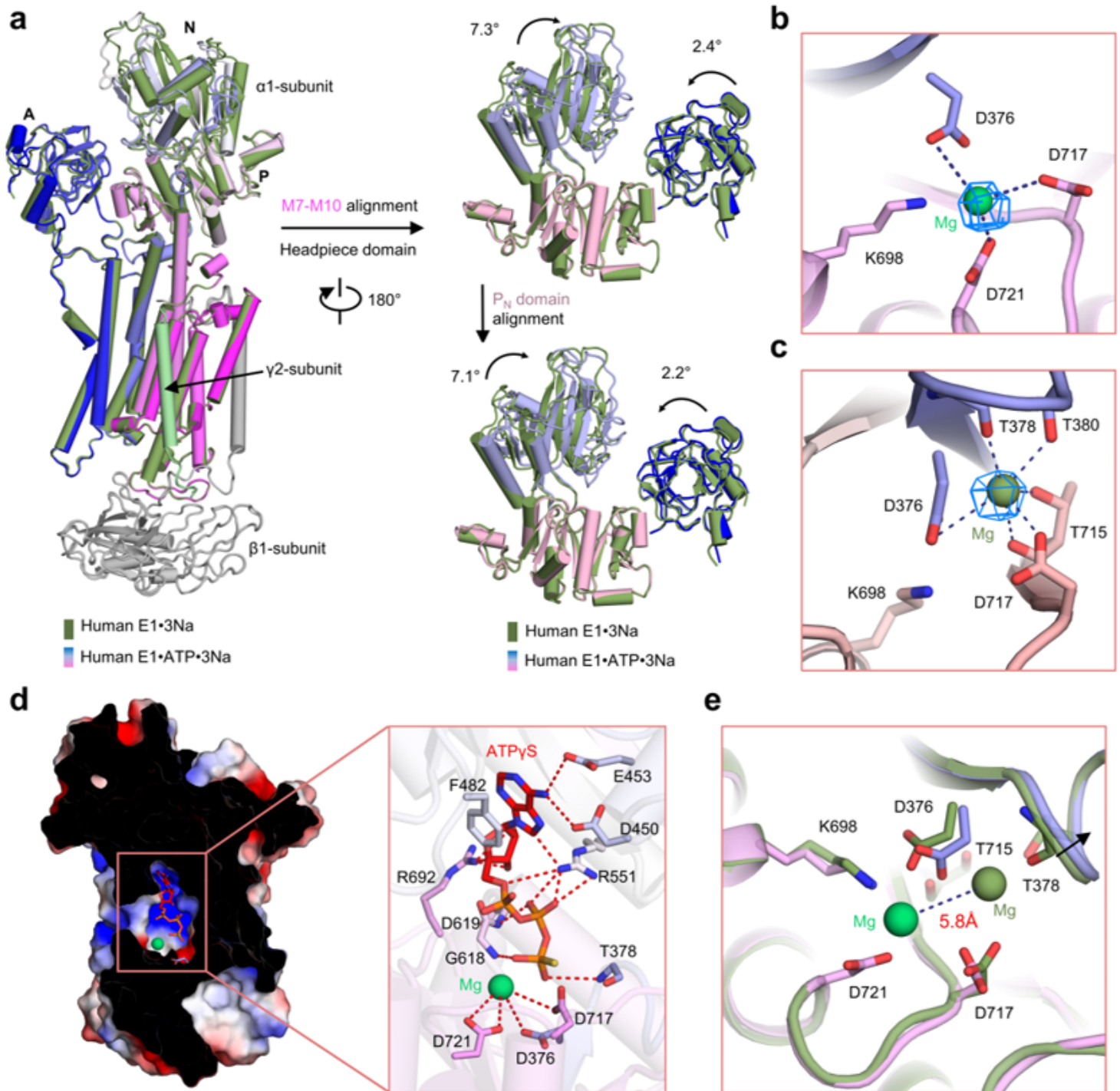


Figure 2

Conformational changes between the E1·3Na-ATP and the E1·3Na state. a, Structural comparison of hNKA between the E1·3Na-ATP state and the E1·3Na state, aligned with M7-M10 or the N-terminal region of the P domain (P_N : 598-710 residues). b, The Mg²⁺ binding site and the phosphorylation site (Asp376) in the E1·3Na-ATP, and in the E1·3Na state (c). d, The ATP binding pocket between the N and the P domain and the key residues around ATPyS. e, Comparison of the Mg²⁺ binding site and the

phosphorylation site (Asp376) between the E1·3Na·ATP state and the E1~P state. Arrow represents the subtle movement of 376DKTGTLT motif.

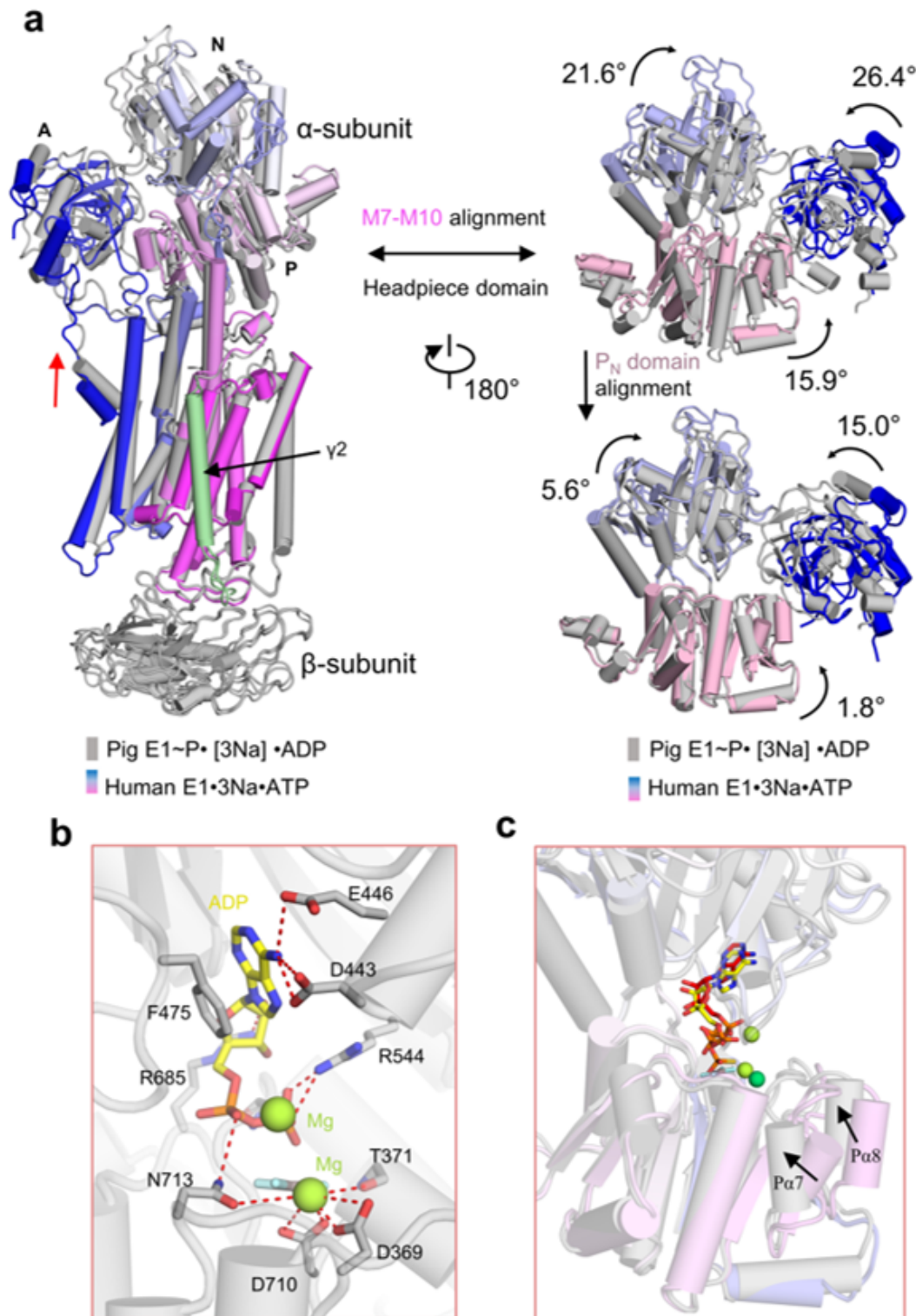


Figure 3

ATP hydrolysis causes cytoplasmic gate closure. a, Structural comparison of the E1·3Na·ATP state with the E1~P·[3Na]·ADP (PDB code: 3WGU) state with the movement of the M1 helix and cytosolic headpiece shown. The structures are superimposed with M7-M10 or PN domain (598-710 residues). Red arrow

represents the close of M1 sliding door. b, The ADP binding pocket between the N and the P domain with the key residues around ADP shown. c, Superimposition of the nucleotide binding sites of E1·3Na·ATP (blue to magenta) and E1~P·[3Na]·ADP (gray), aligned with the PN domain.

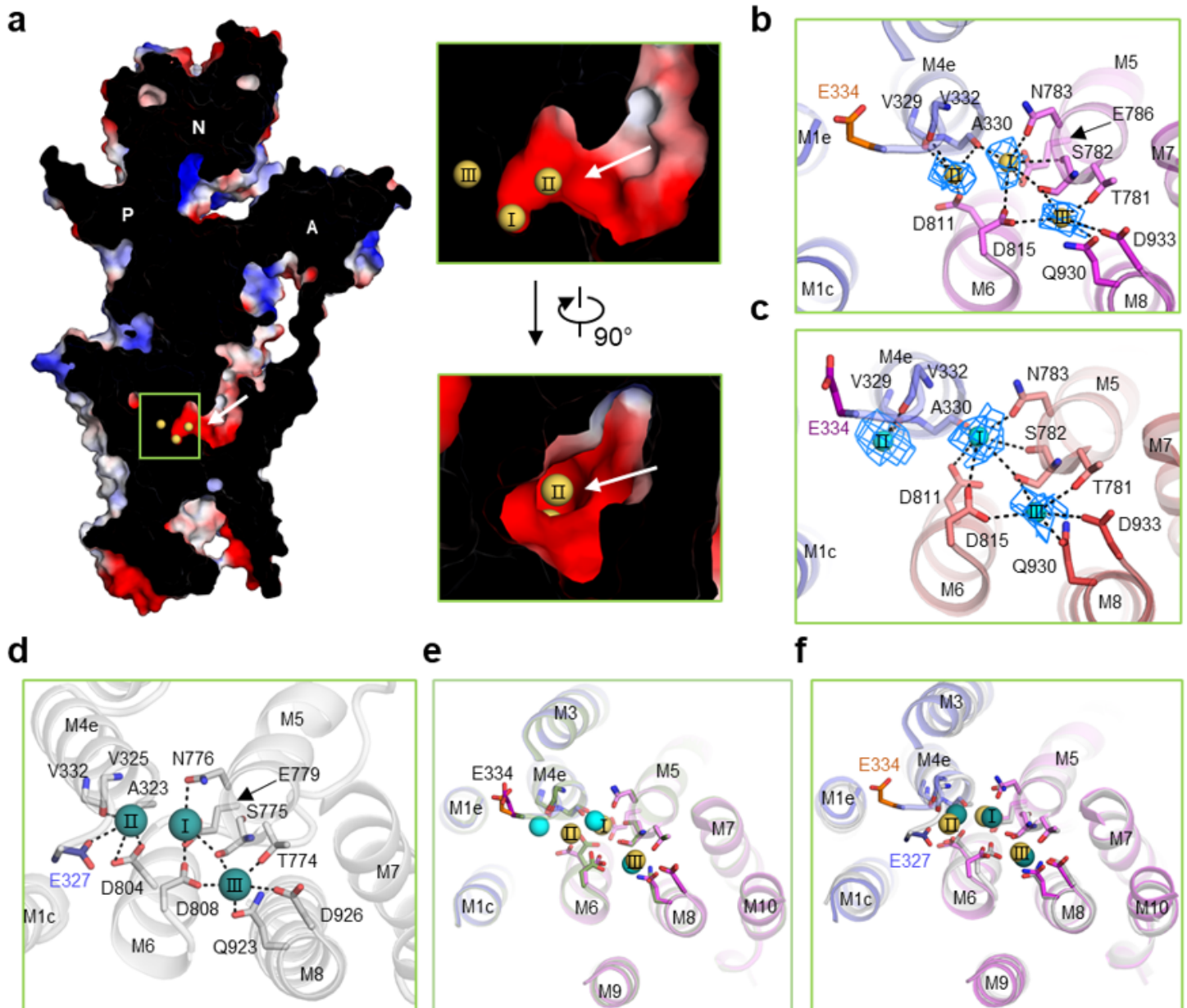


Figure 4

Sodium ion access path and binding sites in different E1 states. a, Cross-section through the Na⁺ entry pathway in E1·3Na·ATP state. Surface representation of hNKA $\alpha 1$ subunit is colored by vacuum electrostatics. Na⁺ are colored yellow. b, c, and d are the transmembrane Na⁺ binding sites in the E1·3Na·ATP, the E1·3Na, and the E1~P·[3Na]·ADP state, with Na⁺ (labeled as I, II and III) shown in yellow, cyan, and deep teal, respectively. The gate residue Glu334 in human (Glu327 in pig) is colored in orange (E1·3Na·ATP), purple (E1·3Na) and slate (E1~P·[3Na]·ADP). e, binding mode comparison of Na⁺ between the E1·3Na·ATP and the E1·3Na state, or f, between the E1·3Na·ATP and the E1~P·[3Na]·ADP state. The structures in e and f are superimposed using M7-M10.

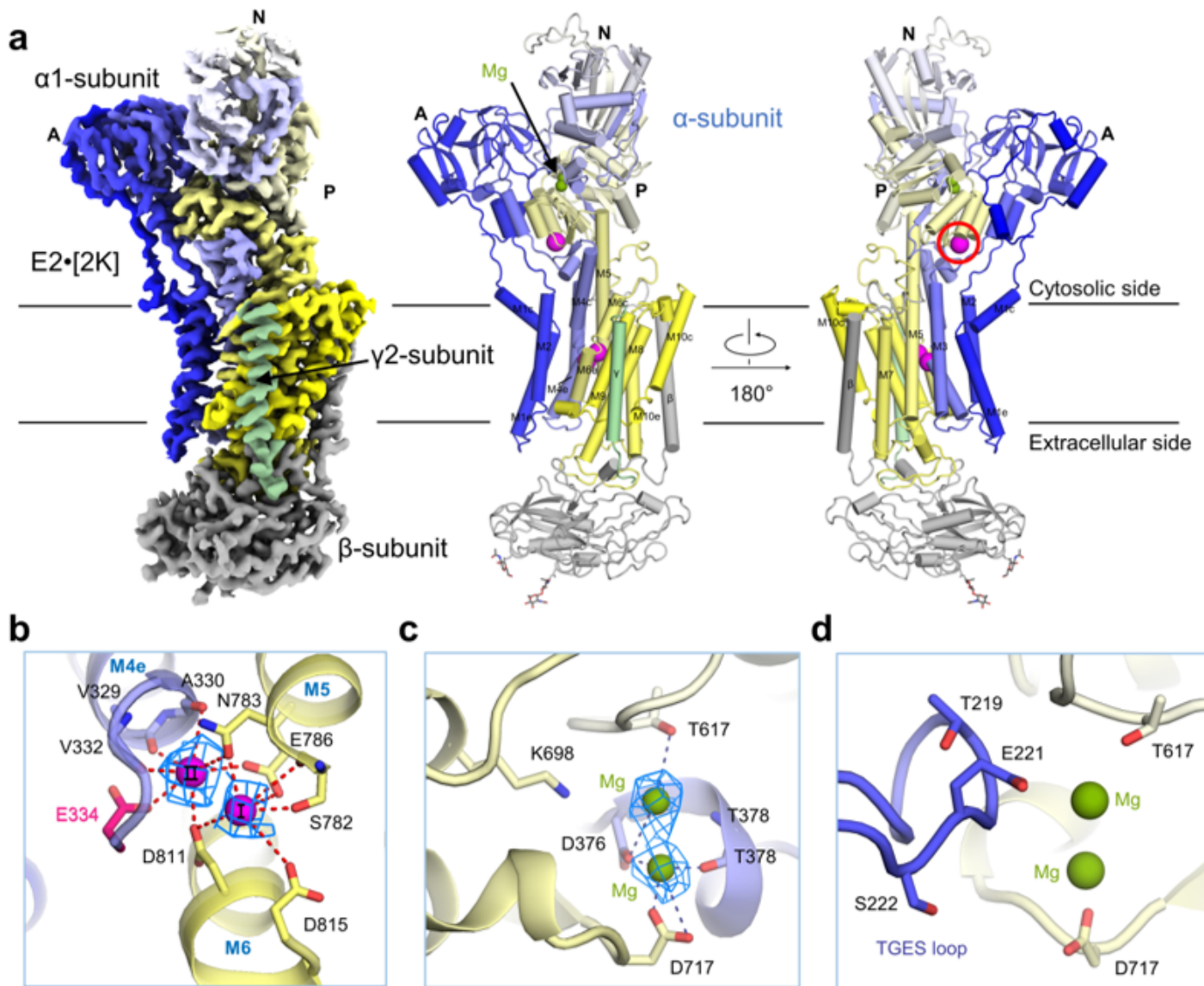


Figure 5

Overall structure of E2·2[K]. a, The overall cryo-EM map of E2·2[K] is shown on the left panel, and two perpendicular views of the overall structure are shown on the middle and right panel. $\alpha 1$ subunit is colored by amino acid sequence with a spectrum from blue to yellow; $\beta 1$ subunit is colored grey; $\gamma 2$ subunit is colored pale green; K ions are colored magenta; Mg^{2+} are colored olive green. The glycosylation moieties are shown as sticks. Red circle represents a cytoplasmic K^+ site (Site C) location. e, extracellular; c, cytosolic; M, transmembrane helix. b, In E2·2[K] state two K^+ are bound in transmembrane K^+ binding sites (I and II). c, Two Mg^{2+} stabilize phosphorylation site (Asp376). d, The hallmark 219TGES motif in the A domain is located near Mg^{2+} sites.

Supplementary Files

This is a list of supplementary files associated with this preprint. Click to download.

- [wholenew20210522.mp4.mp4](#)
- [SI0524.docx](#)